

1        **A COMPREHENSIVE ANALYSIS OF TRENDS IN EXTREME**  
2        **PRECIPITATION OVER SOUTHEASTERN COAST OF BRAZIL**

3  
4        **SHORT TITLE: EXTREME PRECIPITATION TRENDS OVER**  
5        **SOUTHEASTERN COAST OF BRAZIL**

6                Marcia T.Zilli<sup>1</sup>, Leila M. V. Carvalho<sup>1,2</sup>, Brant Liebmann<sup>3</sup>, Maria A. Silva Dias<sup>4</sup>

7        <sup>1</sup> Department of Geography, University of California, Santa Barbara, CA, USA

8        <sup>2</sup> Earth Research Institute, University of California, Santa Barbara, CA, USA

9        <sup>3</sup> CIRES, National Oceanic and Atmospheric Administration (NOAA), Boulder, CO, USA

10        <sup>4</sup> Department of Atmospheric Sciences, University of Sao Paulo, SP, Brazil.

11        **Corresponding author:** Marcia T Zilli (mzilli@umail.ucsb.edu), Department of Geography, 1832

12        Ellison Hall, University of California, Santa Barbara, CA. 93106-4060 Phone: (805) 637-7806.

1   **ABSTRACT**

2   Southeast Brazil (SE Brazil) is the most densely populated region in Brazil. Previous studies have shown  
3   evidence of positive trends in average precipitation and extreme events in a few locations, suggesting the  
4   increase in rainfall related hazards with potential impacts to urbanized areas of SE Brazil. This study  
5   provides a comprehensive analysis of the spatial variability of trends in extreme precipitation over SE  
6   Brazil focusing on regional and local scales. We examine two daily rainfall datasets with more than 70  
7   years of data: individual stations and gridded observed precipitation data. Our results indicate that the  
8   frequency of both rainy days and extreme daily precipitation events have increased in Sao Paulo state.  
9   Conversely, precipitation has become more concentrated in fewer events in Rio de Janeiro and Espirito  
10   Santo states where both data sets indicate positive trends in the intensity of extreme daily rainfall. The  
11   increase in frequency and intensity of extreme events have both contributed to positive trends in total  
12   seasonal and average daily precipitation over Sao Paulo. Additionally, individual stations indicate  
13   negative trends in the number of light rainy days over large urbanized areas in the state of Sao Paulo. The  
14   spatial patterns of trends indicate that they are influenced by the proximity of large urban centers and  
15   topographic features, and also suggest variations and changes in the major climatic systems affecting  
16   precipitation regimes over SE.

17   **Keywords:** precipitation trends; extreme events; spatial variability of precipitation; observed  
18   precipitation; Southeast Brazil.

## 1. Introduction

Southeast Brazil (SE Brazil), with more than 85 million inhabitants, is the most populous region in the country and is responsible for about 55.2% of the gross national product (IBGE, 2012). The dominant climatic feature is the pronounced seasonal cycle in precipitation, moisture and circulation, controlled by the South American Monsoon System (SAMS) (Zhou and Lau, 2001). The South Atlantic Convergence Zone (SACZ), one of the main features of the SAMS, is characterized by a northwest-southeast rain band extending from the Amazon across SE Brazil toward the subtropical South Atlantic (Kodama, 1992) and is related to the occurrence of extreme precipitation events in SE Brazil (Liebmann *et al.*, 2001; Carvalho *et al.*, 2002; Carvalho *et al.*, 2004; Muza *et al.*, 2009; Cavalcanti, 2012). The economic and strategic position of SE Brazil brings forth concerns about environmental security, especially population exposure to precipitation-related disasters such as floods and landslides. This region exhibits one of the largest urban growth rates in Brazil (IBGE, 2012) and changes in precipitation regimes, particularly extremes, may dramatically increase population's vulnerability and negatively impact adaptation capability to projected future climate change scenarios by the middle and end of the 21<sup>st</sup> century (IPCC, 2013).

In 2013, the Intergovernmental Panel on Climate Change (IPCC) released its Fifth Assessment Report (AR5) showing that the increase in global temperature since the last century is certain both over land and ocean, with the last three decades being warmer than any other previous decades in instrumental records (Hartmann *et al.*, 2013). Although the warming of the troposphere is expected to increase the capacity of the atmosphere to retain moisture following the Clausius-Clapeyron relation, implications for changes in rainfall are much more complex and spatially non-uniform (Held and Soden, 2006). Future scenarios of climate change for South America indicate an intensification of monsoonal circulation and precipitation south of 20°S (Kitoh *et al.*, 2013; Jones and Carvalho, 2013) and a southward displacement of the mean position of the SACZ (Seth *et al.*, 2010; Junquas *et al.*, 2012; Cavalcanti and Shimizu, 2012) by the end of the 21<sup>st</sup> century comparatively to the 20<sup>th</sup> century. However, these studies also indicate that large uncertainties still remain regarding the magnitude and signal of precipitation changes over SE Brazil (Kitoh *et al.*, 2013; Carvalho and Jones, 2013; Jones and Carvalho, 2013).

Previous observational studies have examined changes in precipitation regimes using rain gauge data at specific locations, most of them limited to a few decades. Over South America, they identified positive trends in precipitation mainly over Southeastern South America (SESA), including some locations in Southern Brazil (Haylock *et al.*, 2006; Marengo *et al.*, 2010). Over SESA, these positive trends were related to intensification of heavy rainfall rather than an increase in the frequency of wet days (Skansi *et al.*, 2013). Over SE Brazil (Figure 1), long-term trends in precipitation were less coherent and exhibited large spatial variability in trends. Despite the observed discrepancies, these studies detected positive trends in rainfall intensity in the states of Rio de Janeiro (RJ; Haylock *et al.*, 2006; Teixeira and Satyamurty, 2011, Dereczynski *et al.*, 2013) and São Paulo (SP; Liebmann *et al.*, 2004; Dufek and Ambrizzi, 2008; Marengo *et al.*, 2010, Marengo *et al.*, 2013; Teixeira and Satyamurty, 2011; Silva Dias *et al.*, 2013, Valverde and Marengo, 2014). Silva Dias *et al.* (2013) observed that trends in heavy rainfall in the city of Sao Paulo were positively correlated to coupled modes of variability in the Pacific (Pacific Decadal Oscillation) and Atlantic (North Atlantic Oscillation) oceans, as well as with the South American Monsoon System (SAMS) and sea surface temperature anomalies along the southeastern coast of Brazil during the wet season.

In addition, some studies have shown an increase in the number of consecutive dry days and a decrease in the number of light rainy days (less than 5mm/day) in the city of Sao Paulo (Xavier *et al.*, 1994; Dufek and Ambrizzi, 2008; Silva Dias *et al.*, 2013; Marengo *et al.*, 2013). Raimundo *et al.* (2014) observed that stations with negative trends in light rainy days were located in more urbanized areas while those located in rural areas to the east, north, and northeast of the metropolitan area showed positive trends for the index.

Most studies that investigated trends in precipitation over SE Brazil were based on rain gauge data with low spatial density (Haylock *et al.*, 2006; Dufek and Ambrizzi, 2008; Marengo *et al.*, 2010; Teixeira and Satyamurty, 2011, Dereczynski *et al.*, 2013) or focused on specific locations such as the metropolitan area of Sao Paulo (Xavier *et al.*, 1994; Sugahara *et al.*, 2009; Silva Dias *et al.*, 2013; Marengo *et al.*, 2013; Raimundo *et al.*, 2014). The objective of this study is to provide a comprehensive analysis of the spatial variability of trends in extreme precipitation over SE Brazil using the longest and spatially densest set of observations available on the coast of Sao Paulo, Rio de Janeiro and Espirito Santo. Here we examined two datasets: rain gauge stations and gridded data. While gridded precipitation

offers an overview of regional and large-scale patterns of precipitation trends, individual stations provide local details and geographical features associated with the observed trends. The rain gauges selected for this study have more than 70 years of daily data with good quality and few missing days. The gridded precipitation dataset is based exclusively on observations, with a good spatial resolution ( $0.5^\circ$ ). The analyses of these data sets allow the detection of trends and respective patterns of spatial variability that have not been shown before for the study region.

We focus our analysis on the coast of SE Brazil because of its economic and social importance and also because of the high uncertainty in future projections of climate change, particularly concerning changes in precipitation regimes (Seth *et al.*, 2010; Kitoh *et al.*, 2013; Junquas *et al.*, 2012; Carvalho and Jones, 2013; Jones and Carvalho, 2013, Dereczynski *et al.*, 2013). This manuscript is organized as follows. Information about the datasets is provided in Section 2. Methodology is described in Section 3. Results are presented in Section 4 and final conclusions in Section 5.

## **2. Data**

We examine precipitation records from two datasets: a daily gridded precipitation dataset from the Physical Sciences Division (PSD), Earth System Research Laboratory (Figure 2; Liebmann and Allured, 2005) and data from individual stations, operated by different Brazilian agencies (Figure 1 and Table 1).

The PSD dataset provides daily precipitation grids from 1938 to 2012, with  $0.5^\circ$  latitude/longitude resolution, and is based on precipitation observed at stations located over most of South America (Liebmann and Allured, 2005). The dataset is composed of daily totals over all valid stations located within a sample radius of  $0.5^\circ$  from the center of the grid point. This assures the inclusion of all stations in at least one grid point. The disadvantage of this method is that a few stations may be included in up to four different grid points, causing additional smoothing of the data and masking out extreme precipitation with a spatial scale smaller than the grid resolution (Liebmann and Allured, 2005). This dataset exhibits variable station density (Figure 2b) and data availability in space and time (Figure 2c). To avoid examining areas with relatively short time series that could misrepresent the extent of actual trends, we first remove all grid points with more than 40% of missing days over the entire period (Figure 2a). In addition, we considered only years with more than 95% of valid days along the wet season (October to

1 March) and grid points with more than 50% of valid seasons (more than 38 years). With these criteria, the  
2 vast majority of grid points over SE Brazil have more than 60 years of data between 1938 and 2012 (dark  
3 shades in Figure 2c). This is the longest daily gridded precipitation available for the region.

4 To further understand trends in heavy precipitation and their spatial variation over the  
5 topographically complex and highly urbanized area of SE Brazil, we also analyze daily precipitation  
6 obtained from 36 rain gauges located on the coast of Sao Paulo (SP), Rio de Janeiro (RJ), Espirito Santo  
7 (ES), and southeastern Minas Gerais (MG) states (Figure 1). These stations are operated by different  
8 Brazilian agencies (Table 1), and are available from the Brazilian National Water Agency website  
9 (Agencia Nacional de Aguas – ANA; <http://hidroweb.ana.gov.br/>). All stations in this data set have at  
10 least 70 years of observations, including the period between 1939 and 1999, with less than 5% missing  
11 days (Table 1). The quality control test carried out in this study checks for outliers based on neighboring  
12 stations, evaluates station metadata to detect changes in station location and days without readings, and  
13 adopts the Rodionov test (Rodionov, 2006) to detect steps and discontinuities in the time series.

14 These raingauge stations are included in the gridded dataset; however, as we will show next,  
15 individual stations are useful to identify local variations in trends, particularly near complex terrain and  
16 urban centers. Urban areas (Figure 1, cross hatching patterns) are delimited using the Global Rural-Urban  
17 Mapping Project Version 1 (GRUMPv1, available at [http://sedac.ciesin.columbia.edu/data/collection/](http://sedac.ciesin.columbia.edu/data/collection/grump-v1)  
18 [grump-v1](http://sedac.ciesin.columbia.edu/data/collection/grump-v1); Balk *et al.*, 2006). This data set considers night light observations collected by a series of US  
19 Department of Defense meteorological satellites as one of the variables in the definition of the urban-  
20 extent grid. The major topographic feature of coastal SE Brazil is the Coastal Range, with average  
21 elevation below 1000m and some peaks above 2000m (Figure 1, shades).

22 This study focuses on the wet season (October to March) and thus most extreme precipitation  
23 events are related to the SACZ activity (Liebmann *et al.*, 2001; Carvalho *et al.*, 2002; Carvalho *et al.*,  
24 2004; Cavalcanti, 2012). Mechanisms related to the observed trends are a subject of our current research  
25 but are not explored in this manuscript.

### 26 **3. Detection and Characterization of Trends**

27 Trends in precipitation can be described as changes in intensity and/or frequency of rainfall  
28 events that may or may not alter the total annual or the mean daily precipitation. To identify these

changes, we derive various indices, based on daily precipitation observations for the wet season (October to March) from both gridded and station data (Table 2): total precipitation (*TotPR*), daily average (*DayPR*), percentage of rainy days (*%PRDay*), number of light rainy days (*NumbLightPR*), maximum seasonal precipitation (*MaxPR*), 95<sup>th</sup> percentile of daily precipitation (95%), frequency of extreme events (*NumbEx*) and intensity of extreme events (*IntEx*).

We define extreme events as days with precipitation equal or greater than the 95<sup>th</sup> percentile, calculated for each station (and grid point) and month separately and using all years of record. The intensity of the events is defined as the amount of rainfall exceeding the 95<sup>th</sup> percentile monthly climatological value, accumulated over the season. The frequency of extremes is estimated as the number of days per season that precipitation exceeds the monthly 95<sup>th</sup> percentile. If extremes occur in two or more consecutive days this sequence is considered as a single event.

For each derived index, we investigate the presence and magnitude of trends by applying the Mann-Kendall trend test (Wilks, 2011) and the Sen's slope test (Sen, 1968; Gocic and Trajkovic, 2013). The Mann-Kendall test identifies whether or not the index exhibits a trend whereas the Sen's slope test estimates the slope of the trend. Both are non-parametric tests and have been largely used in studies of tendency in atmospheric and hydrological variables (Dufek and Ambrizzi, 2008; Marengo *et al.*, 2010; Ghosh *et al.*, 2012; Gocic and Trajkovic, 2013). The Mann-Kendal statistic *S* is estimated as (Wilks, 2011):

$$S = \sum_{i=1}^{n-1} \sum_{j=i+1}^n \text{sgn}(x_j - x_i) \quad (1)$$

where *n* is the number of data points; *x* is each of the measurements at different time steps *i* and *j*, with *i* ≠ *j*; and *sgn*(.) is defined as:

$$\text{sgn} = \begin{cases} 1, & \text{if } (x_j - x_i) > 0 \\ 0, & \text{if } (x_j - x_i) = 0 \\ -1, & \text{if } (x_j - x_i) < 0 \end{cases} \quad (2)$$

The Mann-Kendall trend test checks the null hypothesis of no trend against the alternative hypothesis of the presence of a trend (Jain and Kumar, 2012); positive (negative) *S* indicates an

- 1 increasing (decreasing) trend. If  $n > 10$ , the  $S$  statistics follows a Gaussian distribution with null average (  
2  $E[S] = 0$ ) and variance:

$$Var[S] = \frac{n(n-1)(2n+5) - \sum_{i=1}^m t_i(t_i-1)(2t_i+5)}{18} \quad (3)$$

- 3 where  $m$  is the number of tied groups (zero difference between compared values) and  $t_i$  is the number of  
4 data points in each tied group (Wilks, 2011). The significance of this trend can be found using  $z$ -scores,  
5 estimated as:

$$z = \begin{cases} \frac{S-1}{\sqrt{Var(S)}}, & S > 0 \\ \frac{S+1}{\sqrt{Var(S)}}, & S < 0 \end{cases} \quad (4)$$

- 6 If  $|z| > z_{\alpha/2}$ , the null hypothesis can be rejected at  $\alpha$  level of significance in a two-sided test  
7 (Jain and Kumar, 2012).

- 8 The Sen's slope estimator test (Gocic and Traijkovic, 2013; Adarsh and Janga Reddy, 2014),  
9 which considers the slopes between all data pairs in the time series, was also applied:

$$Q_i = \frac{x_j - x_k}{j - k} \text{ for } i = 1, 2, \dots, N \quad (5)$$

- 10 where  $N$  is the number of different pairs of observations so that  $N = \frac{n(n-1)}{2}$ ;  $x_j$  and  $x_k$  are data values  
11 at time  $j$  and  $k$ , with  $j > k$ . The slope estimator is computed by considering the median value of all  
12 ranked  $Q_{(i)}$ :

$$Q_{med} = \begin{cases} Q_{[(N+1)/2]} & , \text{if } N \text{ is odd} \\ \frac{Q_{[N/2]} + Q_{[(N+2)/2]}}{2} & , \text{if } N \text{ is even} \end{cases} \quad (6)$$

- 13 where  $Q_{med}$  represents the steepness of the trend, with positive (negative) values representing positive  
14 (negative) trends. The confidence interval for this test is estimated by  $C_\alpha = z_{1-\alpha/2} \sqrt{Var[S]}$ , where



1  $Var[S]$  is estimated by eq. 3, and  $z_{1-\alpha/2}$  is defined from the standard normal distribution. The confidence  
2 interval is:

$$Q_{min} = Q_{(M_1)} \wedge Q_{max} = Q_{(M_2+1)} \quad (7)$$

$$M_1 = \frac{N - C_\alpha}{2} \wedge M_2 = \frac{N + C_\alpha}{2} \quad (8)$$

3 where  $Q_{min}$  and  $Q_{max}$  are the lower and upper limits of the confidence interval. The slope  $Q_{med}$  is  
4 statistically different from zero if the two limits ( $Q_{min}$  and  $Q_{max}$ ) have similar sign.

5 Before applying these tests, we also check the autocorrelation of each time series. Whenever  
6 significance level of the lag-1 autocorrelation coefficient ( $r_1$ ) is above 0.95, the Mann-Kendall variance is

7 adjusted by  $Var^{\hat{c}}[S] = Var[S] \frac{1+r_1}{1-r_1}$ , as suggested by Wilks (2011).

8 Here, trends are considered statistically significant based on the statistic  $S$  for the Mann-Kendall  
9 test (Eq. 1) at 10% significance level. The confidence interval for the Sen's slope is also 10%.

## 10 4. Results

### 11 4.1. Climatology of the Indices

12 We first calculate the climatology of all indices evaluated in this paper (Figure 3) at those grid  
13 points with less than 40% missing data (Figure 2a), effectively restricting the analysis to eastern Brazil.  
14 Table 2 summarizes the indices investigated in this study and shows the climatological spatial average of  
15 each index over all grid points between 49°W to 40°W and 25°S to 20°S, representing SE Brazil. The  
16 average rainfall over SE Brazil during the wet season is 1122.7mm (*TotPR*; Figure 3a), and the mean wet  
17 day precipitation rate is about 9mm/day (*DayPR*; Figure 3b). *%PRDay* and *NumbLightPR* (Figures 3c and  
18 3d) emphasize the large number of rainy days per season. Figure 3c shows that approximately 60% of the  
19 days (equivalent to 110 out of 182 days) have precipitation above 1mm/day. About 43% of the rainy days  
20 (i.e., 47 out of 110 rainy days; Figure 3d) are associated with precipitation rates between 1 and 5 mm/day.

21 The *MaxPR* and *95%* (Figures 3e and 3f) are also large over SE Brazil and both have spatial  
22 distribution similar to the *DayPR* spatial pattern, and all three indices are consistent with the

1 climatological position of the SACZ. Over SE Brazil, *MaxPR* is, on average, 52mm/day and 95% is  
2 29.1mm/day. The average *NumbEx* is 7 events per season (Figure 3g), with *IntEx* larger than  
3 90mm/season (Figure 3h).

4 Large *DayPR*, *MaxPR*, 95% and *IntEx* (Figures 3b, 3e, 3f and 3i) are also observed over  
5 Southern Brazil. Intense precipitation in this region results from the interplay of phenomena on a broad  
6 range of spatiotemporal scales and this discussion is beyond the scope of the present article.

#### 7 4.2. Trends in gridded dataset

8 The gridded dataset indicates a significant increase ( $p < 0.1$ ) in *TotPR* over SP and South Brazil  
9 (Figure 4a). Over SP, positive trends in *TotPR* are collocated with positive significant trends ( $p < 0.1$ ) in  
10 *DayPR*, *MaxPR*, 95%, *NumbEx*, and *IntEx* (Figures 4b, 4e, 4f, 4g and 4h, stippled areas). These positive  
11 trends suggest that extreme daily precipitation events are becoming more intense (increase in *IntEx*,  
12 *MaxPR* and 95%) and more frequent (increase in *NumbEx*), affecting the total seasonal precipitation  
13 (*TotPR*) and the daily average (*DayPR*). Conversely, there are significant negative trends ( $p < 0.1$ ) in  
14 *%PRDay* and *NumbLightPR* (Figures 4c and 4d) in the state, indicating a decrease in the number of rainy  
15 days (days with precipitation above 1mm) and light rain days (days with precipitation between 1 and 5  
16 mm). Both results are in agreement with previous studies (Xavier *et al.*, 1994; Haylock *et al.*, 2006;  
17 Dufek and Ambrizzi, 2008; Sugahara *et al.*, 2009; Marengo *et al.*, 2010; Teixeira and Satyamurty, 2011;  
18 Silva Dias *et al.*, 2013; Skansi *et al.*, 2013; Raimundo *et al.*, 2014, Valverde and Marengo, 2014).

19 Interestingly, the area with positive trends in *TotPR*, *DayPR*, *MaxPR*, and 95%, over SP is  
20 located south of the area of climatological maximum for each index (compare Figures 3 and 4). The  
21 climatological maximum for these indices is collocated with the average position of the SACZ (Figure 3),  
22 indicating that trends observed in the indices could be related to a progressive southwestward  
23 displacement of the SACZ. Previous studies that investigated multimodel projections of climate change in  
24 the wet season precipitation regimes using the Coupled Model Intercomparison Project (CMIP) phase-3  
25 (Seth *et al.*, 2010) and more recently CMIP phase-5 dataset (Jones and Carvalho, 2013) and have  
26 indicated similar displacement of the SACZ, suggesting that the observed trends could be the signal of a  
27 regional response in precipitation caused by the radiative forcing due to global warming.

Over northern SE Brazil, negative trends in *TotPR*, *DayPR*, *MaxPR*, *95%*, *NumbEx* and *IntEx* (Figures 4a, 4b, 4e-4h) and positive trends in *%PRDay* and *NumbLightPR* (Figures 4c and 4d) are opposite to the observed trends over SP. We speculate that this drying tendency, which is associated with decrease in the intensity and frequency of extreme events, is related to the wetting tendency farther south, both a consequence of a southwestward displacement of the SACZ.

We also observe the presence of significant ( $p < 0.1$ ) positive trends over RJ for *TotPR*, *%PRDay*, *MaxPR*, *95%*, *NumbEx*, and *IntEx* indices (Figures 4a, 4c, 4e-h). The *DayPR* and *NumbLightPR* also show positive, but non-significant, trends in the region. These trends are observed over the northern portion of the state and indicate that extreme events are becoming more frequent and intense over the region. Dereczynski *et al.* (2013) identified similar trends; however their study focused only on the city of Rio de Janeiro. Our analysis, based on gridded data with longer time series, detected that these trends are broader and extend over the northern portion of RJ.

#### 4.3. Trends at individual stations

To detail the spatial variability of trends over coastal areas of SE Brazil, we examined precipitation data from 36 individual stations with the longest available records in the region (Figure 1). Positive significant trends ( $p < 0.1$ ) in *TotPR* are identified in 5 stations whereas only 2 stations showed negative and significant ( $p < 0.1$ ) trends (Figure 5a). The *DayPR* also exhibits similar spatial variability of trends: 22 stations indicate positive trends although only 8 stations are statistically significant ( $p < 0.1$ ; Figure 5b). These trends in *DayPR* occur mostly in RJ, where the *%PRDay* and *NumbLightPR* (Figures 5c and 5d) show negative significant trends, indicating a tendency for fewer but more intense precipitation events over that area.

Further south, over SP, positive trends in *TotPR* and *DayPR* (Figures 5a and 5b) are observed along with positive trends in *%PRDay* (Figure 5c), in agreement with previous investigations based on individual stations (Dufek and Ambrizzi, 2008; Teixeira and Satyamurty, 2011). Trends in *NumbLightPR* (Figure 5d) are more complex, with negative significant trends observed over urbanized areas around the city of Sao Paulo as indicated in Xavier *et al.* (1994) and Marengo *et al.* (2013). Stations over rural areas show positive significant trends for the number of light rainy days, as observed by Raimundo *et al.* (2014).

Trends in intense precipitation events are examined based on 4 indices: *MaxPR*, *95%*, *NumbEx* and *IntEx* (Figures 5e-5h). Positive trends in all four indices are observed in at least 24 out of the 36 stations for each index, and the trend in each index was statistically significant ( $p < 0.1$ ) in at least 6 stations. The majority of stations with significant trends are located over RJ and over urban areas of SP. These results reinforce the previous results (Figure 5) that the increase in *DayPR* over RJ is related to more intense and more frequent heavy precipitation days, with a decrease in *%PRDay* and *NumbLightPR*.

To compare our results with previous studies, we focus our analysis on two stations located in the Metropolitan Area of Sao Paulo (stations 30 and 31 in Figure 1 and Table 1). The precipitation record from station 31 has been examined in many previous studies due to its proximity to a large urban center, long record and excellent quality control of data (e.g., Xavier *et al.*, 1994; Sugahara *et al.*, 2009; Silva Dias *et al.*, 2013; Marengo *et al.*, 2013; Raimundo *et al.*, 2014). Our analysis indicate positive significant trends in *TotPR*, *DayPR*, *MaxPR*, *NumbEx*, and *IntEx* (Figures 5a, 5b, 5e, 5g and 5h), and negative trend in *NumbLightPR* (Figure 5d), in agreement with those previous studies.

#### 4.4. Comparison between gridded data and individual station trends

Overall, trends observed for the gridded dataset are similar to those for individual stations. This is not completely surprising as all stations used in this study were included in the gridded data. However, some local discrepancies do exist. The most noticeable differences are observed for *%PRDay* and *NumbLightPR* over the northern RJ. Gridded data indicate positive trends for both indices, significant for *%PRDay* (Figures 4c and 4d), while most stations over this area show significant negative trends for both indices (Figures 5c and 5d). These discrepancies are likely related to the averaging method utilized in the gridded dataset. In regions with complex topography, precipitation exhibits large spatial variability, with large amounts concentrated in small areas where orographic lifting may increase the probability of convective rainfall relative to neighboring stations. However, when averaging precipitation records into a  $0.5^\circ$  grid, these few stations likely contribute to the relative increase in the average number of rainy days. In these cases individual stations provide a more realistic characterization of spatial variability of rainfall trends.

Over SP, trends in *NumbLightPR* are also different between data sets, with the gridded dataset indicating a negative trend over the entire state (statistically significant over central SP; Figure 4d) while

1 stations indicate negative trends only in two stations located in urbanized areas (Figure 5d). Other stations  
2 located in rural areas of SP show positive trends, indicating that 0.5° grid is not sufficient to resolve  
3 difference between urban and rural areas.

4 The analysis of both datasets also reveals a spatial pattern of trends over SP to RJ. While over SP  
5 there is an increase in total precipitation and daily rates (*TotPR* and *DayPR*, Figures 4a-b, 5a-b) caused by  
6 more intense and frequent extreme precipitation events (*MaxPR*, 95%, *NumbEx* and *IntEX*; Figures 4e-4h  
7 and 5e-h), over RJ the intense events are becoming stronger and more frequent (*MaxPR*, 95%, *NumbEx*  
8 and *IntEX*; Figures 4e-4h and 5e-5h), but the number of days with precipitation is decreasing  
9 (*NumbLightPR* and *%PRDay*, Figures 4c-d and 5c-d).

## 10 **5. Discussion and Conclusions**

11 Previous studies have shown compelling evidence that precipitation and its extremes have  
12 changed in the last decades in SE Brazil. These studies, however, were based on spatially averaged  
13 precipitation with relatively coarse resolution (Liebmann *et al.*, 2004; Teixeira and Satyamurty, 2011), or  
14 based on stations located in SP (Haylock *et al.*, 2006; Dufek and Ambrizzi, 2008; Sugahara *et al.*, 2009;  
15 Marengo *et al.*, 2010, Marengo *et al.*, 2013; Silva Dias *et al.*, 2013). The present study develops a  
16 comprehensive analysis of rainfall and its extremes using the most up to date and longest rainfall gauge  
17 records available in SP, RJ, ES and MG. Our major objective is to properly characterize patterns of  
18 changes in intensity and frequency of both light and extreme rainfall events. The trends detected using  
19 these observational precipitation dataset provide strong evidence that changes predicted for future  
20 scenarios of climate change are already occurring.

21 Although the gridded and gauge datasets used here are not independent, trend analysis using  
22 gridded precipitation identified regional patterns of changes in rainfall, whereas station records improved  
23 the identification of local variations in these patterns, particularly near complex terrain and major urban  
24 centers. Mapping trends in SE Brazil has significant economic and social impacts for the country. High  
25 urban population density, inappropriate occupation of risk areas in RJ, SP and MG, and positive trends in  
26 extreme precipitation suggest an increasing exposure to rain-related disasters in these regions.

27 Table 3 summarizes the qualitative interpretation of the main results observed in this study. Over  
28 SP, both datasets indicate an increase in total seasonal and average daily precipitation and suggests that

1 these changes are related to an increase in the frequency and intensity of extreme events, consistent with  
2 previous studies. Additionally, the gridded dataset indicates that the areas with significant trends for these  
3 indices are located southwest of the climatological maximum of rainfall. Since SACZ is the most  
4 important climatological phenomenon modulating precipitation in the region, a plausible explanation for  
5 the positive trend in total precipitation over SP is a southwestward displacement of the SACZ in recent  
6 decades, as previously speculated in Liebmann *et al.* (2004) and suggested in coupled climate model  
7 simulations of future scenarios of climate change in South America discussed in Seth *et al* (2010) and  
8 Jones and Carvalho (2013). Our results, based on observed precipitation, suggest that poleward  
9 displacement of the SACZ is already evident in historical data.

10 Farther north, in RJ and ES, both datasets agree that positive trends in the daily average are  
11 related to trends in intensity and frequency of extreme precipitation days (Table 3). Individual stations  
12 also reveal negative trends in the percentage of rainy days and in the number of light rainy days. These  
13 trends, not evident in the gridded data, indicate changes in the frequency and intensity of precipitation  
14 events, with larger accumulation occurring in fewer rainy days. Dereczynski *et al.* (2013) identified  
15 similar trends in future scenarios of climate change for the city of Rio de Janeiro. Our results confirm that  
16 these trends are already detectable in historical data and show that these trends actually extend to larger  
17 areas north of the state.

18 Therefore, while over SP there is an increase in the number of rainy days and in the frequency  
19 and intensity of extreme events, over RJ and ES we observe a negative trend in the frequency of rainy  
20 days, with precipitation concentrated in fewer and more intense events. These results are consistent with  
21 the hypothesis of the southwestward displacement of the SACZ.

22 Tropical South America has undergone a rapid warming in the last 5 decades, a trend that is  
23 expected to continue and increase by the end of the 21<sup>st</sup> century (Carvalho and Jones, 2013). It has been  
24 argued that the reduction in the frequency of rainy days along the margin of the convective zones, such as  
25 the SACZ, is one of the consequences of the changes in moisture spatial variability in a warmer  
26 atmosphere (Chou and Neelin, 2004; Held and Solden, 2006; Lintner and Neelin, 2010; Ma *et al.*, 2011).  
27 According to them, warmer temperatures would increase the saturation vapor pressure, increasing the  
28 moisture necessary to reach saturation. In the core of convective regions, there is always enough moisture  
29 to meet this higher threshold for precipitation. However, along the convective margins, the moisture

availability might not be enough to reach the new level of saturation, since these areas receive most of their influx from more stable areas, in this case the ocean. In addition, moisture in convective margins is also exported to the region of strong convection, reducing even more the moisture availability and, consequently, increasing stability and decreasing precipitation events in these regions. We speculate that the observed reduction in the number of rainy events over RJ and ES could be related to the warming and subsequent changes in saturation water vapor along the northern margin of the SACZ. The observed positive trends in extreme daily precipitation could be related to thermodynamic effects such as an increase in convective instability. Nevertheless, many other dynamic and thermodynamic mechanisms, combined to environmental changes such as the effect of rapid urbanization and land-use and change, could also have played a significant role in the observed trends in precipitation. Therefore, further investigation is necessary to properly recognize the underlying dynamical and physical mechanisms responsible for the observed trends in precipitation, and ultimately mitigate climate change impacts and prevent water-related disasters in densely populated areas in SP and RJ.

## Acknowledgements

The following Brazilian agencies provided the individual station data: Agencia Nacional de Aguas (ANA), Servico Geologico Brasileiro (CPRM), Instituto Nacional de Meteorologia (INMET); LIGHT; FURNAS Centrais Hidreletricas, Fundacao Centro Tecnologico de Hidraulica (FCTH); Departamento de Aguas e Energia Eletrica (DAEE); and COHIDRO Consultoria, Estudos e Projetos. The urban extend information was a courtesy of the Center for International Earth Science Information Network - CIESIN - Columbia University, International Food Policy Research Institute - IFPRI, The World Bank, and Centro Internacional de Agricultura Tropical - CIAT. 2011. Global Rural-Urban Mapping Project, Version 1 (GRUMPv1): Urban Extents Grid. Palisades, NY: NASA Socioeconomic Data and Applications Center (SEDAC). <http://dx.doi.org/10.7927/H4GH9FVG>, accessed February, 25, 2015. M. Zilli acknowledges the Brazilian National Council for Scientific and Technological Development (CNPq) for the financial support through the Science without Borders Program (process number 202691/2011-0). L. Carvalho thanks National Oceanic and Atmospheric Administration (NOAA) support (NA10OAR4310170). MAF. Silva Dias acknowledges FAPESP support (2009/15235-8 and 2013/105014-0).

## 1    6. References

- 2    Adarsh S, Janga Reddy M. 2014. Trend analysis of rainfall in four meteorological subdivisions of  
3    southern India using nonparametric methods and discrete wavelet analysis, *Int J Climatol* **35**: 1107-1124.  
4    doi: 10.1002/joc.4042.
- 5    Balk DL, Deichmann U, Yetman G, Pozzi F, Hay SI, Nelson A. 2006. Determining global population  
6    distribution: methods, applications and data. *Advances in Parasitology* **62**: 119-156. doi: 10.1016/S0065-  
7    308X(05)62004-0.
- 8    Carvalho LMV, Jones C. 2013. CMIP5 simulations of low-level tropospheric temperature and moisture  
9    over tropical Americas. *J. Climate* **26**: 6257-6286. doi: 10.1175/JCLI-D-12-00532.1.
- 10    Carvalho LMV, Jones C, Liebmann B. 2002. Extreme precipitation events in southeastern South America  
11    and large-scale convective patterns in the South Atlantic Convergence Zone. *J Climate* **15**: 2377-2394.
- 12    Carvalho LMV, Jones C, Liebmann B. 2004. The South Atlantic Convergence Zone: intensity, form,  
13    persistence and relationships with intraseasonal to interannual activity and extreme rainfall. *J Climate* **17**:  
14    88-108.
- 15    Cavalcanti IFA. 2012. Large scale and synoptic features associated with extreme precipitation over South  
16    America: a review and case studies for the first decade of the 21st century. *Atmospheric Research* **118**:  
17    27-40. doi: 10.1016/j.atmosres.2012.06.012.
- 18    Cavalcanti IFA, Shimizu MH. 2012. Climate fields over South America and variability of SACZ and PSA  
19    in HadGEM-ES. *Am. J. Clim. Change* **1**: 132-144. doi: 10.4236/ajcc.2012.13011.
- 20    Chou C, Neelin JD. 2004. Mechanisms of global warming impacts on regional tropical precipitation. *J*  
21    *Climate* **17**: 2688-2701.
- 22    Dereczynski CP, Luiz Silva W, Marengo JA. 2013. Detection and Projections of Climate Change in Rio  
23    de Janeiro, Brazil. *American Journal of Climate Change* **2**: 25-33. doi: 10.4236/ajcc.2013.21003.
- 24    Dufek AS, Ambrizzi T. 2008. Precipitation variability in São Paulo state, Brazil. *Theor Appl Climatol* **93**:  
25    167-178. doi: 10.1007/s00704-007-0348-7.
- 26    Ghosh S, Das D, Kao SC, Ganguly AR. 2012. Lack of uniform trends but increasing spatial variability in  
27    observed Indian rainfall extremes. *Nature Climate Change* **2**: 86-91. doi: 10.1038/NCLIMATE1327.
- 28    Gocic M, Trajkovic S. 2013. Analysis of changes in meteorological variables using Mann-Kendall and  
29    Sen's slope estimator statistical test in Serbia. *Global and Planetary Change* **100**: 172-182. doi:  
30    10.1016/j.gloplacha.2012.10.014.
- 31    Hartmann DL *et al.* 2013. Observations: atmosphere and surface. In: Stocker TF *et al.* (eds.): Climate  
32    change 2013: the physical science basis. Contribution of working group I to the fifth assessment report of  
33    the Intergovernmental Panel on Climate Change, Chapter 2. Cambridge University Press, New York, pp  
34    159-254.
- 35    Haylock MR *et al.* 2006. Trends in total and extremes South American rainfall in 1960-2000 and links  
36    with sea surface temperature. *J Climate* **19**: 1490-1512. doi: 10.1175/JCLI3695.1.
- 37    Held IM, Soden BJ. 2006. Robust response of the hydrological cycle to global warming. *J Climate* **19**:  
38    5686-5699.
- 39    IBGE. 2012. Contas regionais do Brasil 2012. Contas Nacionais número 42. [ftp://ftp.ibge.gov.br/  
40    Contas\\_Regionais/2012/pdf/](ftp://ftp.ibge.gov.br/Contas_Regionais/2012/pdf/). Accessed 3 Mar 2015. (in Portuguese)



1 IPCC, 2013. Climate Change 2013: The Physical Science Basis. Contribution of Working Group I to the  
2 Fifth Assessment Report of the Intergovernmental Panel on Climate Change. In: Stocker, TF *et al.*, (eds.).  
3 Cambridge University Press, New York, 1535 pp

4 Jain SK, Kumar V. 2012. Trend analysis of rainfall and temperature data for India. *Current Science* **102**:  
5 37-49.

6 Jones C, Carvalho LMV. 2013. Climate change in the South American Monsoon System: present climate  
7 and CMIP5 projections. *J Climate* **26**: 6660–6678. doi: 10.1175/JCLI-D-12-00412.1.

8 Junquas C, Vera C, Li L, LeTreut H. 2012. Summer precipitation variability over southeastern South  
9 America in a global warming scenario. *Clim Dyn* **38**: 1867-188. doi: 10.1007/s00382-011-1141-y.

10 Kitoh A, Endo H, Krishna Kumar K, Cavalcanti IFA, Goswami P, Zhou T. 2013. Monsoons in a  
11 changing world: regional perspective in a global context. *J Geophys Res* **118**: 3053-3065. doi:  
12 10.1002/jgrd.50258

13 Kodama Y-M. 1992. Large-scale common features of subtropical precipitation zones (the Baiu Frontal  
14 Zone, the SPCZ and the SACZ) part I: Characteristics of subtropical frontal zones. *J Meteorol Soc Jpn*  
15 **70**: 813-835.

16 Liebmann B, Allured D. 2005. Daily precipitation grids for South America. *Bull Amer Meteor Soc* **86**:  
17 1567-1570.

18 Liebmann B, Jones C, Carvalho LMV. 2001. Interannual variability of daily extreme precipitation events  
19 in the state of Sao Paulo, Brazil. *J Climate* **14**: 208-218.

20 Liebmann B, Vera CS, Carvalho LMV, Camilloni A, Hoerling MP, Allured D, Barros VR, Baez J,  
21 Bidegain M. 2004. An observed trend in central South American precipitation. *J Climate* **17**: 4357-4367.

22 Lintner BR, Neelin JD. 2010. Tropical South America-Atlantic sector convective margins and their  
23 relationship to low-level inflow. *J Climate* **23**: 2671-2685. doi:10.1175/2009JCLI3301.1.

24 Ma H-Y, Ji X, Neelin JD, Mechoso CR. 2011. Mechanisms for precipitation variability of the eastern  
25 Brazil/SACZ convective margin. *J Climate* **24**: 3445-3456. doi: 10.1175/2011JCLI4070.1.

26 Marengo JA, Rusticucci M, Penalba O, Renom M. 2010. An intercomparison of observed and simulated  
27 extreme rainfall and temperature events during the last half of the twentieth century: part 2: historical  
28 trends, *Climatic Change* **98**: 509-529. doi: 10.1007/s10584-009-9743-7.

29 Marengo JA, Valverde MC, Obregon GO. 2013. Observed and projected changes in rainfall extremes in  
30 the Metropolitan Area of São Paulo. *Climate Research* **57**: 61-72. doi: 10.3354/cr01160.

31 Muza MN, Carvalho LMV, Jones C, Liebmann B. 2009. Intraseasonal and interannual variability of  
32 extreme dry and wet events over southeastern South America and the subtropical Atlantic during austral  
33 summer. *J Climate* **22**: 1682-1699. doi: 10.1175/2008JCLI2257.1.

34 Raimundo CC, Sansigolo CA, Molion LCB. 2014. Trends of rainfall classes in the metropolitan region of  
35 Sao Paulo. *Rev Bras Meteor* **29**: 397-408. doi: 10.1590/s0102-778620130655 (in Portuguese).

36 Rodionov, S. 2006. Use of prewhitening in climate regime shift detection. *Geoph Res Let* **33**: L12707-4.  
37 doi: 10.1029/2006GL025904.

38 Sen PK. 1968. Estimates of the regression coefficient based on Kendall's Tau. *J Amer Statist Assoc* **63**:  
39 1379-1389.

40 Seth A, Rojas M, Rauscher SA. 2010. CMIP3 projected changes in the annual cycle of the South  
41 American Monsoon. *Climatic Change* **98**: 331–357. doi: 10.1007/s10584-009-9736-6.

- 1 Silva Dias MAF, Dias J, Carvalho LMV, Freitas ED, Silva Dias PL. 2013. Changes in extreme daily  
2 rainfall for Sao Paulo, Brazil. *Climatic Change* **116**: 705-722. doi: 10.1007/s10584-012-0504-7.
- 3 Skansi MM, *et al.* 2013. Warming and wetting signals emerging from analysis of changes in climate  
4 extreme indices over South America. *Global and Planetary Change* **100**: 295-307. doi:  
5 10.1016/j.gloplacha.2012.11.004.
- 6 Sugahara S, Rocha RP, Silveira R. 2009. Non-stationary frequency analysis of extreme daily rainfall in  
7 Sao Paulo, Brazil. *Int J Climatol* **29**: 1339-1349. doi: 10.1002/joc.1760.
- 8 Teixeira MS, Satyamurty P. 2011. Trends in the frequency of intense precipitation events in Southern and  
9 Southeastern Brazil during 1960-2004. *J Climate* **24**: 1913-1921. doi: 10.1175/2011JCLI3511.1.
- 10 USGS. 2004. Shuttle Radar Topography Mission, 30 Arc Second, Global Land Cover Facility, University  
11 of Maryland, College Park, Maryland, February 2000.
- 12 Valverde, MC, Marengo JA. 2014. Extreme Rainfall Indices in the Hydrographic Basins of Brazil. *Open*  
13 *Journal of Modern Hydrology* **4**: 10-26. doi: <http://dx.doi.org/10.4236/ojmh.2014.41002>
- 14 Wilks DS. 2011. *Statistical methods in the atmospheric sciences*. Vol. 100. Academic Press.
- 15 Xavier TMBS, Xavier AFS, Silva Dias MAF. 1994. Evolução da precipitação diária num ambiente  
16 urbano: o caso da cidade de São Paulo. *Rev Bras Meteor* **9**: 44-53. (in Portuguese).
- 17 Zhou J, Lau K-M. 2001. Principal modes of interannual and decadal variability of summer rainfall over  
18 South America. *Int J Climatol* **21**: 1623-1644. doi: 10.1002/joc.700.

## 19 **Figures and Table**

20 **Fig. 1** Inset: Location of SE Brazil (shaded) and study area (dashed line) in Brazil. Main map: Location  
21 of the study area (dashed line) at SE Brazil; stations analyzed (“•”); shades: local topography  
22 (1km resolution DEM from SRTM; USGS 2004); cross hatching: urban area (GRUMPv1 dataset,  
23 Balk et al. 2006). Information about stations is provided in Table 1. This figure is available in  
24 color online at [wileyonlinelibrary.com/journal/joc](http://wileyonlinelibrary.com/journal/joc)

25 **Fig. 2** Gridded dataset: % of missing days (a); average number of stations per grid point (b); and number  
26 of valid years per grid point (c). (b) and (c): only grid points with less than 40% missing days.  
27 Dashed line: study area. Gray contour: states of SE Brazil. Stars: Sao Paulo (23.6°S, 46.6°W) and  
28 Rio de Janeiro (22.9°S, 43.2°W). This figure is available in color online at  
29 [wileyonlinelibrary.com/journal/joc](http://wileyonlinelibrary.com/journal/joc)

30 **Fig. 3** Wet season climatology for gridded data: *TotPR* (a), *DayPR* (b), *%PRDay* (c), *NumbLightPR* (d),  
31 *MaxPR* (e), *95%* (f); *NumbEx* (g) and *IntEx* (h). Dashed line: study area. Gray contour: states of  
32 SE Brazil. Stars: Sao Paulo (23.6°S, 46.6°W) and Rio de Janeiro (22.9°S, 43.2°W). This figure is  
33 available in color online at [wileyonlinelibrary.com/journal/joc](http://wileyonlinelibrary.com/journal/joc)

34 **Fig. 4** Trends in gridded dataset for wet season: *TotPR* (a), *DayPR* (b), *%PRDay* (c), *NumbLightPR* (d),  
35 *MaxPR* (e), *95%* (f); *NumbEx* (g) and *IntEx* (h). Blue (red) areas: positive (negative) trends (Sen’s  
36 slope); stippled areas: significant trends ( $p < 0.1$ ). Gray contour: states of SE Brazil. Stars: Sao  
37 Paulo (23.6°S, 46.6°W) and Rio de Janeiro (22.9°S, 43.2°W). This figure is available in color  
38 online at [wileyonlinelibrary.com/journal/joc](http://wileyonlinelibrary.com/journal/joc)

1 **Fig. 5** Trends in station data for wet season: *TotPR* (a), *DayPR* (b), *%PRDay* (c), *NumbLightPR* (d),  
2 *MaxPR* (e), *95%* (f); *NumbEx* (g) and *IntEx* (h). “+” (“-”): positive (negative) trends; blue (red)  
3 symbols: positive (negative) significant trends ( $p < 0.1$ ); shades: local topography; dashed line:  
4 study area. In (d) cross hatching: urban areas (source: GRUMPv1 dataset, Balk et al. 2006). This  
5 figure is available in color online at [wileyonlinelibrary.com/journal/joc](http://wileyonlinelibrary.com/journal/joc)  
6

7 **Table 1** Stations analyzed, latitude, longitude, height, city where located, time range, percentage of  
8 missing, and source institution. The location of these stations is in Figure 1

9 **Table 2** Precipitation indices, acronyms, their definition, and mean value for the wet season (based on  
10 the gridded data averaged over the entire period for all grid points over coastal SE Brazil -  
11 49°W to 40°W and 25°S to 20°S)

12 **Table 3** Trends in each index considering both dataset, for the states of RJ and ES, SP, and the  
13 Metropolitan Area of Sao Paulo (MASP). Symbols: positive (▲), negative (▼) or no  
14 significant (■) trends.

**Table 1** Stations analyzed, latitude, longitude, height, city where located, time range, percentage of missing, and source institution. The location of these stations is in Figure 1

ID	Station	Lat (°S)	Lon (° W)	Height (m)	City	First Year	Last Year	Missing (%)	Operated by
1	02041001	-20.77	-41.68	576	Guaçu, ES	1939	2013	1.18	ANA <sup>a</sup> /CPRM <sup>b</sup>
2	02041002	-20.61	-41.20	107	Castelo, ES	1939	2013	1.35	ANA/CPRM
3	02141003	-21.49	-41.61	20	Campos dos Goytacazes, RJ	1939	2013	0.16	ANA/CPRM
4	02141014	-21.21	-41.46	59	Mimoso do Sul, ES	1937	2013	0.31	ANA/CPRM
5	02141044	-21.75	-41.33	25	Campos dos Goytacazes, RJ	1912	2009	2.66	INMET <sup>c</sup>
6	02141045	-21.20	-41.90	124	Itaperuna, RJ	1922	2009	1.60	INMET
7	02142002	-21.15	-42.22	177	Patrocínio do Muriaé, MG	1935	2013	0.17	ANA/CPRM
8	02142022	-21.95	-42.36	376	Cantagalo, RJ	1939	2013	0.40	ANA/CPRM
9	02143000	-21.31	-43.20	512	Rio Pombo, MG	1935	2013	2.19	ANA/CPRM
10	02242027	-22.20	-42.90	650	Teresópolis, RJ	1936	2013	0.12	ANA/CPRM
11	02243010	-22.49	-43.15	1085	Petrópolis, RJ	1938	2013	0.23	ANA/CPRM
12	02243011	-22.44	-43.17	704	Petrópolis, RJ	1938	2013	0.43	ANA/CPRM
13	02243015	-22.13	-43.15	270	Tres Rios, RJ	1936	2013	0.26	ANA/CPRM
14	02244004	-22.58	-44.97	520	Cruzeiro, SP	1929	2004	1.21	LIGHT <sup>d</sup>
15	02244010	-22.69	-44.98	550	Cachoeira Paulista, SP	1935	2013	1.90	ANA/CPRM
16	02244035	-22.15	-44.09	530	S. Rita de Jacutinga, MG	1935	2013	1.33	ANA/CPRM
17	02244036	-22.24	-44.26	550	Passa Vinte, MG	1935	2013	0.80	ANA/CPRM
18	02244047	-22.33	-44.54	1030	Resende, RJ	1937	2013	1.17	ANA/CPRM
19	02244092	-22.48	-44.45	440	Resende, RJ	1925	2009	3.17	INMET
20	02244097	-22.77	-44.09	500	Pinheiral, RJ	1915	2004	0.28	LIGHT
21	02244133	-22.68	-44.32	460	Bananal, SP	1937	2013	3.26	FURNAS <sup>e</sup>
22	02245032	-22.81	-45.18	519	Guaratinguetá, SP	1930	2012	0.49	FURNAS
23	02245048	-22.91	-45.47	524	Pindamonhangaba, SP	1932	2012	1.76	ANA/CPRM
24	02245055	-23.00	-45.04	790	Cunha, SP	1935	2013	0.74	ANA/CPRM
25	02345047	-23.53	-45.85	770	Salesópolis, SP	1927	2004	1.17	FCTH <sup>f</sup> /DAEE <sup>g</sup>
26	02345048	-23.57	-45.83	790	Salesópolis, SP	1928	2004	0.22	FCTH/DAEE
27	02345063	-23.08	-45.71	545	Caçapava, SP	1929	2013	2.94	ANA/CPRM
28	02345065	-23.22	-45.32	760	S. L. do Paraitinga, SP	1935	2013	1.43	ANA/CPRM
29	02345067	-23.33	-45.14	888	S. L. do Paraitinga, SP	1936	2013	1.02	ANA/CPRM
30	02346045	-23.53	-46.63	730	São Paulo, SP	1888	1999	2.13	FCTH/DAEE
31	02346059	-23.65	-46.63	780	São Paulo, SP	1933	2004	0.01	FCTH/DAEE
32	02346099	-23.42	-46.02	567	Guararema, SP	1929	2003	0.97	ANA
33	02348033	-23.56	-48.39	580	Angatuba, SP	1938	2013	3.54	ANA/COHIDRO <sup>h</sup>
34	02447043	-24.25	-47.38	18	Miracatu, SP	1939	2013	1.25	ANA/COHIDRO
35	02447045	-24.29	-47.18	42	Itariri, SP	1937	2013	2.31	ANA/COHIDRO
36	02447046	-24.32	-47.62	15	Juquiá, SP	1937	2006	2.70	ANA/COHIDRO

<sup>a</sup> ANA – Agencia Nacional de Aguas

<sup>b</sup> CPRM – Serviço Geológico Brasileiro

<sup>c</sup> INMET – Instituto Nacional de Meteorologia

<sup>d</sup> LIGHT

<sup>e</sup> FURNAS Centrais Hidrelétricas

<sup>f</sup> FCTH – Fundação Centro Tecnológico de Hidráulica

<sup>g</sup> DAEE – Departamento de Aguas e Energia Elétrica

<sup>h</sup> COHIDRO Consultoria, Estudos e Projetos

**Table 2** Precipitation indices, acronyms, their definition and climatological average over SE (averaged on 49°W to 40°W and 25°S to 20°S)

INDEX	ACRONYM	DEFINITION	SE AVERAGE
Total precipitation	TotPR	Total precipitation accumulated along the wet season	1122.7 mm
Daily average	DayPR	Average daily precipitation for the wet season, considering only days with precipitation above 1mm.	9.7 mm/day
Percentage of rainy days	%PRDay	Number of days with precipitation above 1mm, divided by the total number of days in the season (182 for the wet season)	63.1%
Number of light rainy days	NumbLightPR	Number of days with precipitation between 1 and 5 mm.	47.4 days
Maximum precipitation	MaxPR	Maximum daily precipitation for each season	52.3 mm/day
95 <sup>th</sup> percentile	95%	Value of the 95 <sup>th</sup> percentile of daily precipitation for each season.	29.1mm/day
Frequency of extreme events	NumbEx	Number of events with daily precipitation above the monthly 95 <sup>th</sup> percentile, per season	7.1 events/year
Intensity of extreme events	IntEx	Exceedance precipitation above the 95 <sup>th</sup> percentile threshold, accumulated during the season	92.6mm

**Table 3** Trends in each index considering both datasets, for the states of RJ and ES, SP, and the Metropolitan Area of Sao Paulo (MASP). Symbols: positive (↗), negative (↘) or no significant (■) trends

INDEX	RJ AND ES	SP	MASP
TotPR	■	↗	↗
DayPR	↗	↗	↗
%PRDay	↘	■	■
NumbLightPR	↘	■	↘
MaxPR	↗	↗	↗
95%	↗	↗	■
NumbEx	↗	↗	↗
IntEx	↗	↗	↗

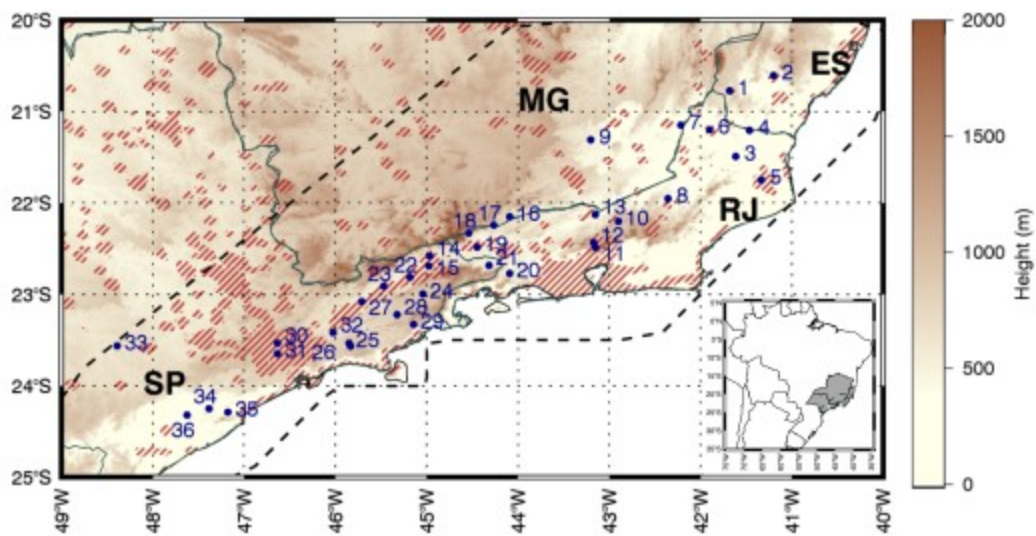


Fig. 1 Inset: Location of SE Brazil (shaded) and study area (dashed line) in Brazil. Main map: Location of the study area (dashed line) at SE Brazil; stations analyzed (“●”); shades: local topography (1km resolution DEM from SRTM; USGS 2004); cross hatching: urban area (GRUMPv1 dataset, Balk et al. 2006). Information about stations is provided in Table 1. This figure is available in color online at [wileyonlinelibrary.com/journal/joc](http://wileyonlinelibrary.com/journal/joc)

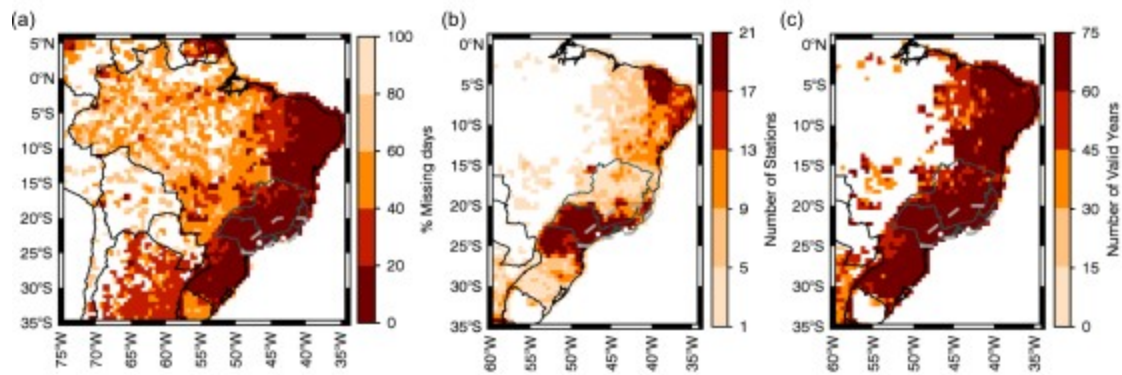


Fig. 2 Gridded dataset: % of missing days (a); average number of stations per grid point (b); and number of valid years per grid point (c). (b) and (c): only grid points with less than 40% missing days. Dashed line: study area. Gray contour: states of SE Brazil. Stars: Sao Paulo (23.6°S, 46.6°W) and Rio de Janeiro (22.9°S, 43.2°W). This figure is available in color online at [wileyonlinelibrary.com/journal/joc](http://wileyonlinelibrary.com/journal/joc)



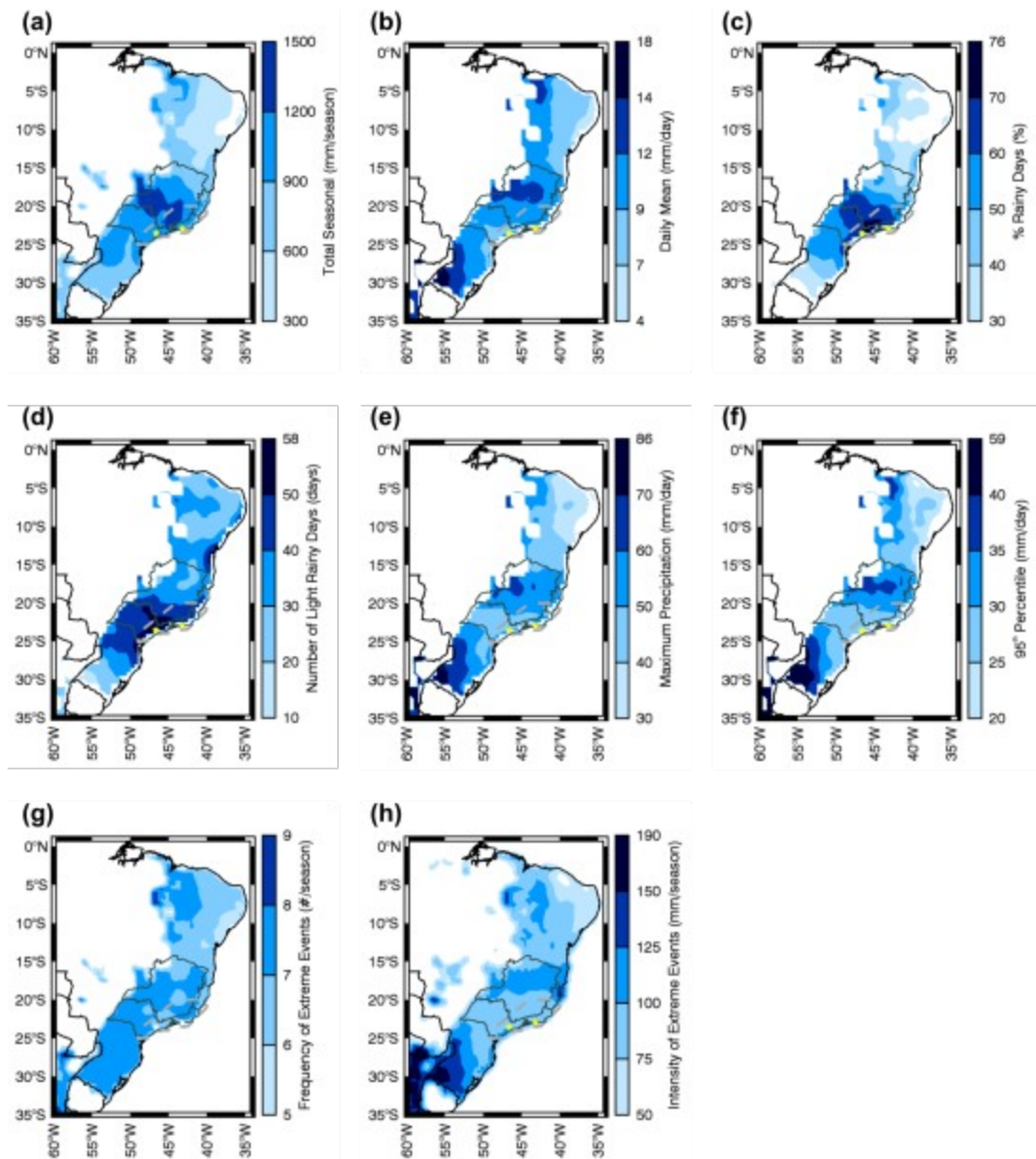


Fig. 3 Wet season climatology for gridded data: *TotPR* (a), *DayPR* (b), *%PRDay* (c), *NumbLightPR* (d), *MaxPR* (e), *95%* (f); *NumbEx* (g) and *IntEx* (h). Dashed line: study area. Gray contour: states of SE Brazil. Stars: Sao Paulo (23.6°S, 46.6°W) and Rio de Janeiro (22.9°S, 43.2°W). This figure is available in color online at [wileyonlinelibrary.com/journal/joc](http://wileyonlinelibrary.com/journal/joc)

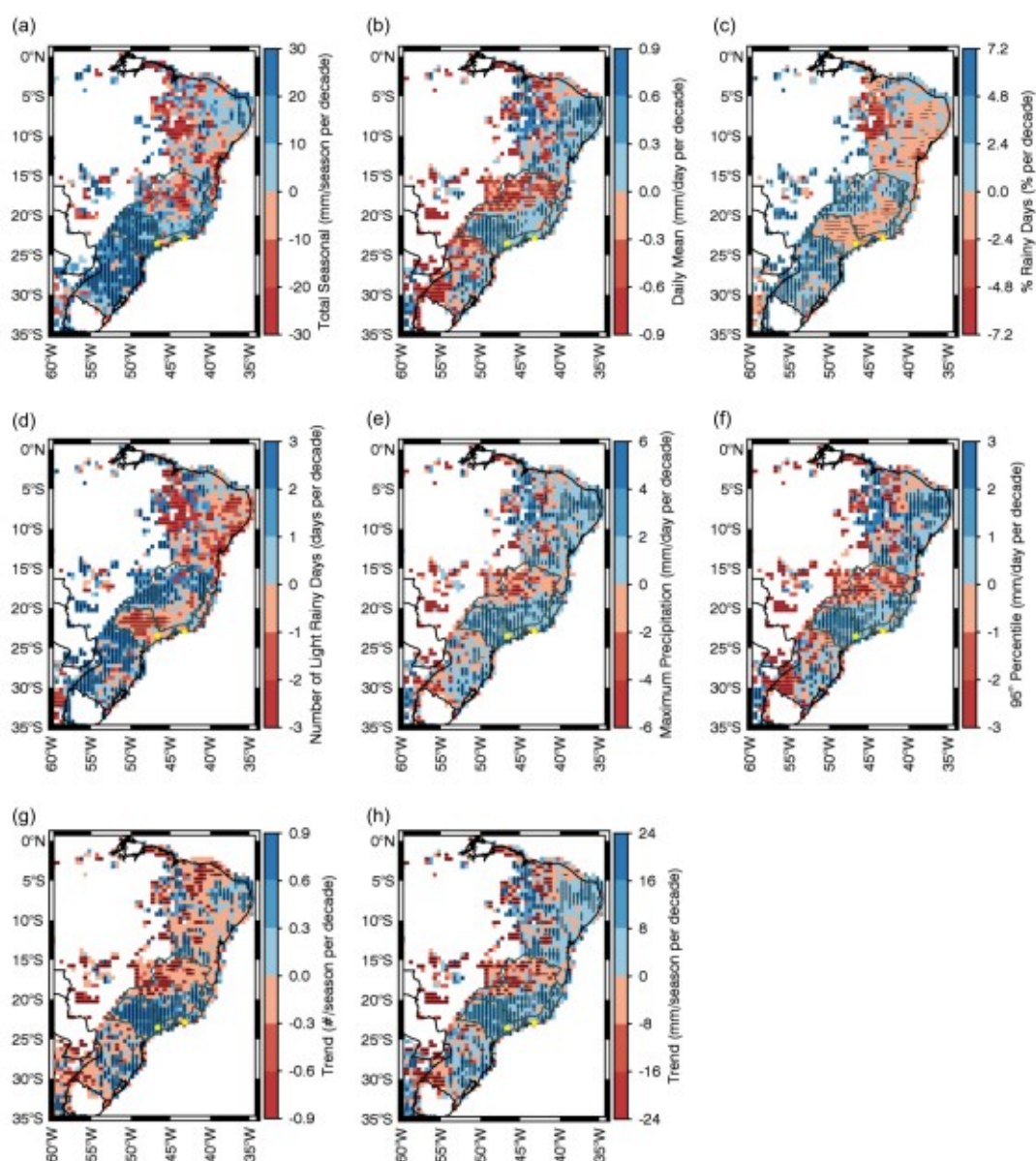


Fig. 4 Trends in gridded dataset for wet season: *TotPR* (a), *DayPR* (b), *%PRDay* (c), *NumbLightPR* (d), *MaxPR* (e), *95%* (f); *NumbEx* (g) and *IntEx* (h). Blue (red) areas: positive (negative) trends (Sen's slope); stippled areas: significant trends ( $p < 0.1$ ). Gray contour: states of SE Brazil. Stars: Sao Paulo (23.6°S, 46.6°W) and Rio de Janeiro (22.9°S, 43.2°W). This figure is available in color online at [wileyonlinelibrary.com/journal/joc](http://wileyonlinelibrary.com/journal/joc)

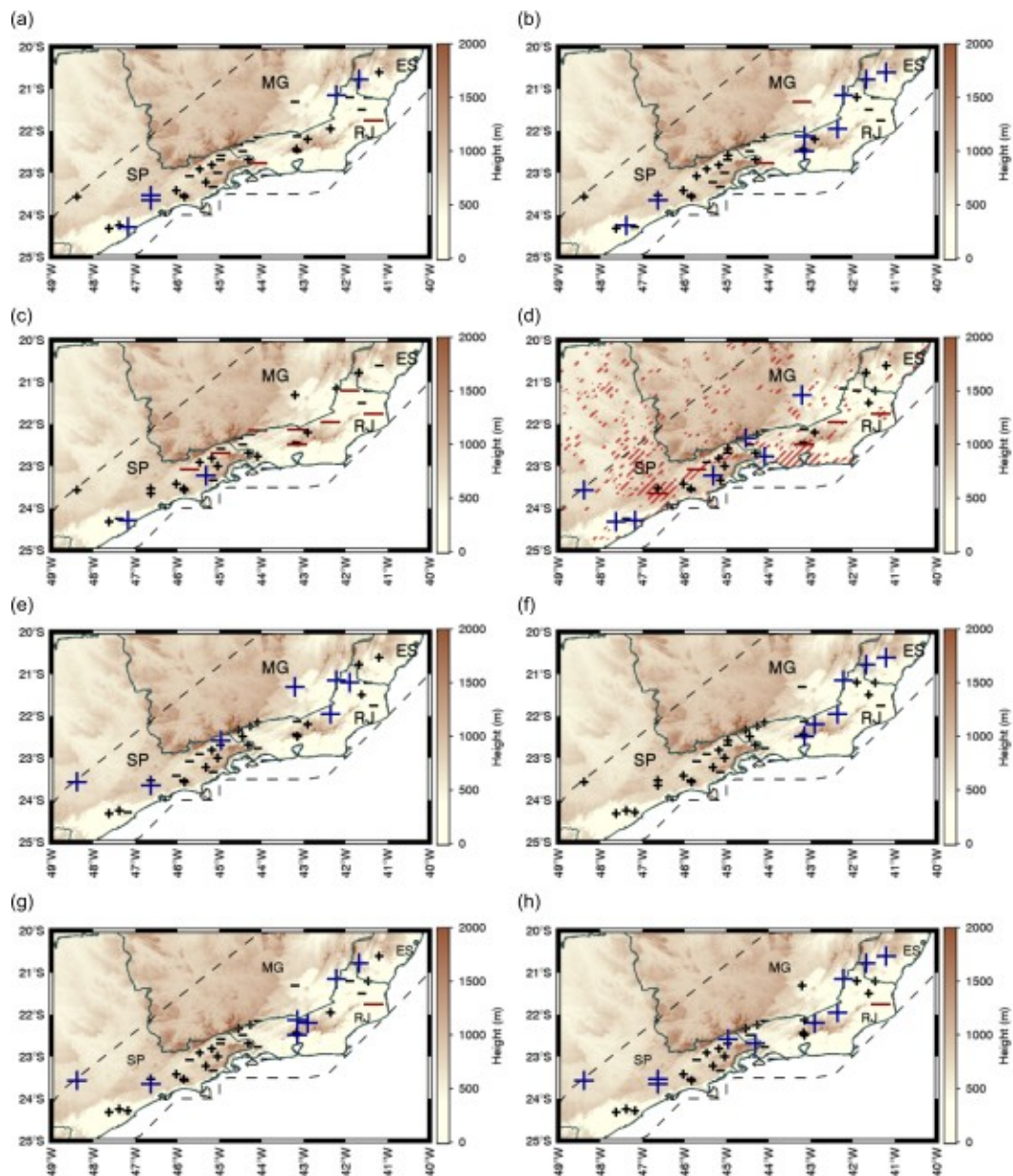


Fig. 5 Trends in station data for wet season: *TotPR* (a), *DayPR* (b), *%PRDay* (c), *NumbLightPR* (d), *MaxPR* (e), *95%* (f); *NumbEx* (g) and *IntEx* (h). "+" ("−"): positive (negative) trends; blue (red) symbols: positive (negative) significant trends ( $p < 0.1$ ); shades: local topography; dashed line: study area. In (d) cross hatching: urban areas (source: GRUMPv1 dataset, Balk et al. 2006). This figure is available in color online at [wileyonlinelibrary.com/journal/joc](http://wileyonlinelibrary.com/journal/joc)